Discrete-time epidemic modeling with chemo-prophylaxis for controlling multidrug-resistant and extensively drug-resistant Tuberculosis in Russia and India

Bouchra Chennaf [✉1] and Mohammed Salah Abdelouahab [1]

[1]Laboratory of mathematics and their interactions, Abdelhafid Boussouf university center, Mila, 43000, Algeria

Abstract. This study presents an enhanced discrete-time epidemic model for tuberculosis (TB) that incorporates the dynamics of multidrug-resistant TB (MDR-TB) and extensively drug-resistant TB (XDR-TB) in the contexts of India and Russia. Despite advancements in TB treatment, the challenge of drug-resistant strains necessitates innovative management strategies. Our analysis, grounded in TB case data from 2000 to 2022, demonstrates that increased chemo-prophylaxis significantly mitigates the progression to resistant TB states, while BCG vaccination effectively boosts immunity and curtails transmission. The findings reveal that India faces a more pressing TB crisis compared to Russia. By employing a discrete VSEIT model, we provide a comprehensive exploration of TB dynamics and the socio-economic implications associated with varying levels of preventative treatments. Sensitivity analyses highlight the importance of optimized treatment regimens, emphasizing the need for public health interventions tailored to local conditions. Overall, this research offers critical insights into the effective control of TB and the management of resistant strains, vital for informing future epidemiological practices.

Keywords: discrete-time model, tuberculosis, global stability, extensively drug-resistant TB, multidrug-resistant TB.

2020 Mathematics Subject Classification: 39A10, 67B89, 92D25. MSC2020

1   Introduction

TB is a bacterial infection that mainly targets the lungs and is transmitted through airborne particles expelled when an infected person coughs, sneezes, or spits. Despite being both preventable and treatable, around one-quarter of the global population carries TB bacteria, with 5–10% eventually developing active TB disease [27].

The complex dynamics of TB transmission and its persistence across various populations call for a thorough understanding and effective control strategies. Mathematical modeling

---

✉Corresponding author. Email: bouchra.chennaf@centre-univ-mila.dz

is a crucial tool for analyzing TB transmission and evaluating potential interventions. The origins of mathematical epidemiology, particularly compartmental models, can be traced back to Sir Ronald Ross, who developed the inaugural mathematical malaria transmission model in 1911 [22].

In epidemiological modeling, differential equations and difference equations are widely used to study infectious diseases. Although differential equations provide more advanced theories and methods for dynamic analysis, recent years have seen a growing interest and significant advancements in discrete epidemic models [1, 26].

The foundational model for understanding TB transmission dynamics was created by Waaler and Anderson [25]. Despite all the great progress in preventing and treating TB, it's still a huge problem worldwide. The emergence of drug-resistant strains like MDR-TB and XDR-TB is a major challenge. Multidrug-resistant tuberculosis (MDR-TB) is characterized by resistance to the two most crucial first-line drugs, isoniazid and rifampicin. Extensively drug-resistant tuberculosis (XDR-TB) shows resistance not only to these first-line drugs but also to at least one fluoroquinolone and one injectable agent [28]. The development of drug resistance (MDR/XDR) can arise from several causes: improper treatment regimens, including the selection of drugs, treatment duration, and correct dosage; patient-related issues such as malabsorption and poor adherence; and program-related factors like unskilled health personnel and irregular drug supply. Indeed, the emergence of MDR-TB is often cited as a sign of the global community's systematic failure to address a curable disease [18].

Gupta et al. [21] expanded the traditional SEIRS epidemiological model to include MDR-TB. Their numerical analysis, both with and without delay, demonstrated that active TB and MDR-TB can persist due to the absence of permanent immunity, as individuals who recover may lose immunity and become susceptible again [9]. To address this, D. B. Kitaro et al. [14] improved the model by incorporating chemoprophylaxis for latent infections and treatments for active TB cases. And in this study, we developed a discrete mathematical model based on an existing continuous mathematical model to illustrate that discrete models are significantly more effective in studying diseases. Consequently, we utilized real data from the two countries most affected by MDR-TB and XDR-TB to ensure the accuracy and relevance of our findings.

Given the importance of discrete-time models in epidemiological research, we developed a discrete-time mathematical model using real TB case data from India and Russia from 2000 to 2022 [23] to explore their dynamics. The main objective is to investigate Euler discretization in an integer context, focusing on parameter estimation and demonstrating the effects of chemoprophylaxis and vaccination on the infected, MDR, and XDR populations. This introduction has briefly reviewed TB models. The remainder of this work is structured as follows: Section 2 details the discrete model formulation and parameter descriptions. Section 3 discusses the mathematical results related to the disease-free equilibrium. Section 4 explores the dynamics of the discrete model in relation to the endemic equilibrium. Section 5 covers parameter estimation, analyzing the sensitivity, and numerical results. Section 6 offers a concise conclusion summarizing the study.

2   Formulation of discrete TB model

In this section, we first present a continuous-time TB model, as detailed in [6], which includes MDR-TB and XDR-TB populations. The aim is to create a model that is easy to analyze, providing a thorough understanding of TB disease dynamics. Additionally, we explore the impact of the chemoprophylaxis rate on infected and resistant TB classes to explain the socio-

economic implications. This analysis helps to understand how varying levels of chemoprophylaxis can influence the spread and resistance patterns of TB, shedding light on the broader socio-economic impact of TB control measures.

TB vaccination is mainly administered through the Bacillus Calmette-Guérin (BCG) vaccine, typically given to infants in countries with high TB incidence. The BCG vaccine provides protection against severe forms of tuberculosis (TB) in children, but it is less effective at preventing the more common pulmonary TB in adults.

Individuals usually contract *Mycobacterium tuberculosis* (MTB) after exposure to those with active TB, entering an exposed phase. Some of these individuals then develop active TB and become infectious. With timely treatment, individuals can recover and move to the treatment category. Those who stop treatment may develop MDR-TB and move into the resistant class. Individuals who recover from MDR-TB also enter the treatment category, but those who do not respond to MDR-TB treatment develop XDR-TB. People who recover from XDR-TB also move into the treatment category.

The population is classified into the following seven categories:

- $V(t)$: Vaccinated at time t.

- $S(t)$: Susceptible at time t.

- $E(t)$: Exposed (not yet infectious) at time t.

- $I(t)$: Infected at time t.

- $D(t)$: Multidrug-resistant TB at time t.

- $X(t)$: Extensively drug-resistant TB at time t.

- $T(t)$: Undergoing treatment at time t.

The behavior of the model is governed by the following system of ordinary differential equations (ODEs):

$$
\begin{aligned}
\frac{dV(t)}{dt} &= \nu\Lambda - (\alpha + \mu)V(t), \\
\frac{dS(t)}{dt} &= (1 - \nu)\Lambda + \alpha V(t) - \beta S(t)I(t) - \mu S(t), \\
\frac{dE(t)}{dt} &= \beta S(t)I(t) - (\epsilon + \mu + \omega)E(t), \\
\frac{dI(t)}{dt} &= \epsilon E(t) - (\tau + \zeta + \gamma + \mu + \sigma)I(t), \\
\frac{dD(t)}{dt} &= \tau I(t) - (\theta + \mu + \delta)D(t), \\
\frac{dX(t)}{dt} &= \zeta I(t) - (\xi + \mu + \eta)X(t), \\
\frac{dT(t)}{dt} &= \gamma I(t) + \omega E(t) + \theta D(t) + \xi X(t) - \mu T(t).
\end{aligned}
\tag{2.1}
$$

with suitable initial conditions that are non-negative:
$V(0) = V_0 \geq 0, S(0) = S_0 \geq 0, E(0) = E_0 \geq 0, I(0) = I_0 \geq 0,$
$D(0) = D_0 \geq 0, X(0) = X_0 \geq 0, T(0) = T_0 \geq 0.$
Parameter Definitions

- Λ : The number of births,

- μ : The natural death rate,

- α : The moving rate from V to S,

- β : The transmission rate,

- γ : The rate of treatment from I,

- ϵ : The progression rate,

- ω : The chemoprophylaxis treatment rate,

- τ : The rate of the resistance to the first line of treatment,

- ζ : The rate of the resistance to the second line of treatment,

- ξ : The Rate of treatment for XDR-TB,

- θ : The rate of treatment for MDR-TB,

- δ : The mortality rate from disease in D,

- σ :The mortality rate from disease in I,

- η : The mortality rate from disease in X,

- ν : The vaccination rate.

Figure 2.1 shows the flow chart for the model. All parameters and variables in system (2.1)
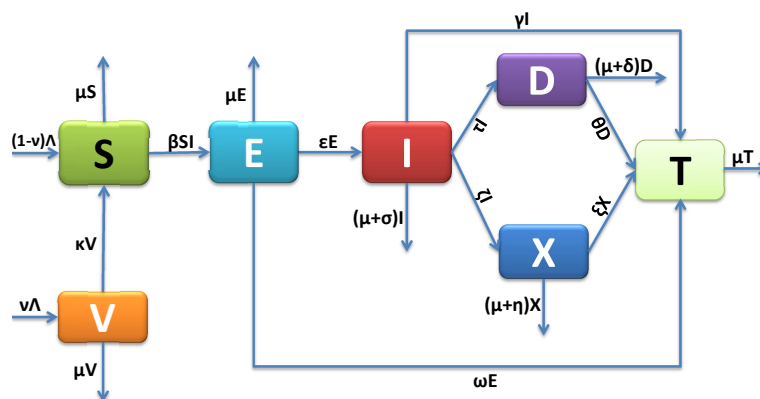

Figure 2.1: Flow chart of the discrete model (2.2)

are nonnegative, reflecting the discrete model's representation of human dynamics. Using

the Euler forward difference scheme [13, 17] with a step size of $h = 1$, the system (2.1) is discretized into the following set of equations:

$$
\begin{aligned}
V_{t+1} &= V_t + \nu\Lambda - (\alpha + \mu)V_t, \\
S_{t+1} &= S_t + (1 - \nu)\Lambda + \alpha V_t - \beta S_t I_t - \mu S_t, \\
E_{t+1} &= E_t + \beta S_t I_t - (\epsilon + \mu + \omega)E_t, \\
I_{t+1} &= I_t + \epsilon E_t - (\tau + \zeta + \gamma + \mu + \sigma)I_t, \\
D_{t+1} &= D_t + \tau I_t - (\theta + \mu + \delta)D_t, \\
X_{t+1} &= X_t + \zeta I_t - (\xi + \mu + \eta)X_t, \\
T_{t+1} &= T_t + \gamma I_t + \omega E_t + \theta D_t + \xi X_t - \mu T_t.
\end{aligned}
\tag{2.2}
$$

with non-negative initial conditions :

$$
V_0 \geq 0, S_0 \geq 0, E_0 \geq 0, I_0 \geq 0, D_0 \geq 0, X_0 \geq 0, T_0 \geq 0.
\tag{2.3}
$$

3 The feasible region

Proposition 3.1. *The feasible region for the discrete tuberculosis model described by system (2.2) is given by:*

$$
\Gamma = \left\{ (V_t, S_t, E_t, I_t, D_t, X_t, T_t) \in \mathbb{R}^7_+ \mid N_t \leq \frac{\Lambda}{\mu} \right\},
$$

and this region is positively invariant.

Proof. Given that

$$
\begin{aligned}
N_{t+1} &= V_{t+1} + S_{t+1} + E_{t+1} + I_{t+1} + D_{t+1} + X_{t+1} + T_{t+1}, \\
&= \Lambda - \mu[V_t + S_t + E_t + I_t + D_t + X_t + T_t] \\
&\quad - \sigma I_t - \delta D_t + \eta X_t + V_t + S_t + E_t + I_t + D_t + X_t + T_t, \\
&= \Lambda - \mu N_t - \sigma I_t - \delta D_t + \eta X_t + N_t, \\
N_{t+1} - N_t &= \Lambda - \mu N_t - \sigma I_t - \delta D_t + \eta X_t, \\
&\leq \Lambda - \mu N_t.
\end{aligned}
\tag{3.1}
$$

For $N_t \leq \dfrac{\Lambda}{\mu}$, we have $N_{t+1} - N_t \leq 0$.

Thus, for $0 \leq N_0 \leq \frac{\Lambda}{\mu}$, it follows that $0 \leq N_t \leq \frac{\Lambda}{\mu}$.

Therefore, the region

$$
\Gamma = \left\{ (V_t, S_t, E_t, I_t, D_t, X_t, T_t) \in \mathbb{R}^7_+ \mid N_t \leq \frac{\Lambda}{\mu} \right\},
$$

is positively invariant. □

4 Disease-free equilibrium

This section focuses on identifying and analyzing a stable solution, known as the Disease-Free Equilibrium (**DFE**) point within the model. .

4.1   Existence of DFE

At the **DFE**, the disease is entirely eradicated from the population. Typically, this equilibrium is achieved by setting the left-hand side of system (2.2) to $(V_t, S_t, E_t, I_t, D_t, X_t, T_t)$ and assigning zero to the variables E, I, D, X, and T.

$$
\begin{aligned}
V_t &= V_t + \nu\Lambda - (\alpha + \mu)V_t, \\
S_t &= S_t + (1 - \nu)\Lambda + \alpha V_t - \beta S_t I_t - \mu S_t, \\
E_t &= E_t + \beta S_t I_t - (\epsilon + \mu + \omega)E_t, \\
I_t &= I_t + \epsilon E_t - (\tau + \zeta + \gamma + \mu + \sigma)I_t, \\
D_t &= D_t + \tau I_t - (\theta + \mu + \delta)D_t, \\
X_t &= X_t + \zeta I_t - (\xi + \mu + \eta)X_t, \\
T_t &= T_t + \gamma I_t + \omega E_t + \theta D_t + \xi X_t - \mu T_t.
\end{aligned}
\tag{4.1}
$$

By solving the system (4.1), the **DFE** is determined as follows:

$$
\textbf{DFE} = (V^*, S^*, E^*, I^*, D^*, X^*, T^*) = \left(\frac{\nu\Lambda}{\alpha + \mu}, \frac{(\alpha + \mu - \mu\nu)\Lambda}{\mu(\alpha + \mu)}, 0, 0, 0, 0, 0 \right),
$$

with $N = \frac{\Lambda}{\mu}$.

4.2   Basic reproduction number $\mathcal{R}_0$

The method outlined in [8, 24] is employed to compute the basic reproduction number $\mathcal{R}_0$ [3, 10] for the discrete TB model. This approach generates essential matrices crucial for determining the threshold parameter, $\mathcal{R}_0$, of model (2.2), given by:

$$
\mathcal{R}_0 = \rho(FV^{-1}).
$$

where FV^{-1} is the next-generation matrix. Matrices F and V are $m \times m$ matrices, where m is the number of infected compartments. The spectral radius of FV^{-1} is denoted by $\rho(FV^{-1})$.

The model equations in (2.2) corresponding to infected classes are:

$$
\begin{aligned}
E_{t+1} &= E_t + \beta S_t I_t - (\epsilon + \mu + \omega)E_t, \\
I_{t+1} &= I_t + \epsilon E_t - (\tau + \zeta + \gamma + \mu + \sigma)I_t, \\
D_{t+1} &= D_t + \tau I_t - (\theta + \mu + \delta)D_t, \\
X_{t+1} &= X_t + \zeta I_t - (\xi + \mu + \eta)X_t.
\end{aligned}
\tag{4.2}
$$

The next-generation matrices F and V are derived as follows:

$$
F = \begin{pmatrix} 0 & \beta S^* & 0 & 0 \\ 0 & 0 & 0 & 0 \\ 0 & 0 & 0 & 0 \\ 0 & 0 & 0 & 0 \end{pmatrix}, \quad
V = \begin{pmatrix} (\epsilon + \mu + \omega) & 0 & 0 & 0 \\ -\epsilon & (\tau + \zeta + \gamma + \mu + \sigma) & 0 & 0 \\ 0 & -\tau & (\theta + \mu + \delta) & 0 \\ 0 & -\zeta & 0 & (\xi + \mu + \eta) \end{pmatrix}.
$$

The matrix FV^{-1} is computed as:

$$
FV^{-1} = \begin{pmatrix} \frac{\epsilon\beta(\alpha + \mu - \mu\nu)\Lambda}{\mu(\alpha + \mu)(\epsilon + \mu + \omega)(\tau + \zeta + \gamma + \mu + \sigma)} & \frac{-\beta(\alpha + \mu - \mu\nu)\Lambda}{\mu(\alpha + \mu)(\tau + \zeta + \gamma + \mu + \sigma)} & 0 & 0 \\ 0 & 0 & 0 & 0 \\ 0 & 0 & 0 & 0 \\ 0 & 0 & 0 & 0 \end{pmatrix}.
$$

The eigenvalues of FV^{-1} are obtained by solving $\left|FV^{-1} - \lambda I_4\right| = 0$, yielding:

$$\lambda_1 = 0, \quad \lambda_2 = 0, \quad \lambda_3 = 0, \quad \text{and}$$

$$\lambda_4 = \frac{\epsilon \beta (\alpha + \mu - \mu \nu) \Lambda}{\mu (\alpha + \mu)(\epsilon + \mu + \omega)(\tau + \zeta + \gamma + \mu + \sigma)},$$

where λ_4 is the dominant eigenvalue. Hence, the basic reproduction number is:

$$\mathcal{R}_0 = \rho(FV^{-1}) = \frac{\epsilon \beta (\alpha + \mu - \mu \nu) \Lambda}{\mu (\alpha + \mu)(\epsilon + \mu + \omega)(\tau + \zeta + \gamma + \mu + \sigma)}.$$

4.3 Global stability investigation of the DFE

Proposition 4.1. *Take the first equation of the model 2.2:*

$$V_{t+1} = V_t + \nu \Lambda - (\alpha + \mu) V_t,$$

If the initial condition $V_0 = 0$ holds, then V_t is increasing for all t and $V_t \leq \frac{\nu \Lambda}{\alpha + \mu}$.

Proof. Given $V_0 = 0$, substitute this into the recurrence relation:

$$V_1 = V_0 + \nu \Lambda - (\alpha + \mu) V_0.$$

Since $V_0 = 0$, this simplifies to:

$$V_1 = \nu \Lambda.$$

Therefore, $V_1 = \nu \Lambda \geq 0$, showing that V_t increases from $t = 0$ to $t = 1$.
Assume $V_t \geq 0$ for some $t \geq 0$. We need to show that $V_{t+1} \geq V_t$.
Using the recurrence relation:

$$V_{t+1} = V_t + \nu \Lambda - (\alpha + \mu) V_t.$$

The difference $V_{t+1} - V_t$ is:

$$V_{t+1} - V_t = \nu \Lambda - (\alpha + \mu) V_t.$$

For $V_{t+1} \geq V_t$, we need:

$$\nu \Lambda - (\alpha + \mu) V_t \geq 0.$$

Rearranging this gives:

$$V_t \leq \frac{\nu \Lambda}{\alpha + \mu}.$$

Given $V_0 = 0$ and $\alpha + \mu > 0$, V_t will remain less than or equal to $\frac{\nu \Lambda}{\alpha + \mu}$ for all t. Therefore, $V_{t+1} \geq V_t$, meaning that V_t is increasing.
To show that V_t is bounded, consider the recurrence relation:

$$V_{t+1} = V_t + \nu \Lambda - (\alpha + \mu) V_t.$$

Rewrite it as:

$$V_{t+1} = V_t \left(1 - (\alpha + \mu)\right) + \nu\Lambda.$$

Define $L = \frac{\nu\Lambda}{\alpha+\mu}$. To see that V_t converges to L, rearrange the equation as:

$$V_{t+1} - L = (V_t - L)\left(1 - (\alpha + \mu)\right).$$

If $\alpha + \mu > 0$, then $1 - (\alpha + \mu) < 1$ and is positive, so V_t approaches L as $t \to \infty$. Specifically, the term $(1 - (\alpha + \mu))$ ensures that the difference $V_t - L$ decreases over time, meaning V_t will be bounded by L. □

The following theorem summarizes the global stability of the **DFE**.

Theorem 4.2. *The model described by system (2.2) is globally asymptotically stable (GAS) at the **DFE** if $\mathcal{R}_0 \leq 1$.*

Proof. To demonstrate GAS of the discrete model given by system (2.2), a Lyapunov function is defined as:

$$F_t = b_1 E_t + b_2 I_t,$$

where the backward difference ΔF is calculated as:

$$\begin{aligned}
\Delta F &= F_{t+1} - F_t, \\
&= b_1(E_{t+1} - E_t) + b_2(I_{t+1} - I_t), \\
&= b_1(E_t + \beta S_t I_t - (\epsilon + \mu + \omega)E_t - E_t) + b_2(I_t + \epsilon E_t - (\tau + \zeta + \gamma + \mu + \sigma)I_t - I_t), \\
&= b_1(\beta S_t I_t - (\epsilon + \mu + \omega)E_t) + b_2(\epsilon E_t - (\tau + \zeta + \gamma + \mu + \sigma)I_t).
\end{aligned}$$

Taking into account that $(S_t \leq N - V_t \leq \frac{\Lambda}{\mu} - \frac{\nu\Lambda}{\alpha+\mu} = \frac{(\alpha+\mu-\mu\nu)\Lambda}{\mu(\alpha+\mu)})$ according to proposition 4.1, one gets

$$\begin{aligned}
\Delta F &\leq b_1(\beta\frac{(\alpha+\mu-\mu\nu)\Lambda}{\mu(\alpha+\mu)}I_t - (\epsilon + \mu + \omega)E_t) + b_2(\epsilon E_t - (\tau + \zeta + \gamma + \mu + \sigma)I_t), \\
&= \left[b_1\beta\frac{(\alpha+\mu-\mu\nu)\Lambda}{\mu(\alpha+\mu)} - b_2(\tau + \zeta + \gamma + \mu + \sigma)\right]I_t + [b_2\epsilon - b_1(\epsilon + \mu + \omega)]E_t, \\
&\leq b_2(\tau + \zeta + \gamma + \mu + \sigma)\left[\frac{b_1\beta(\alpha+\mu-\mu\nu)\Lambda}{\mu(\alpha+\mu)b_2(\tau + \zeta + \gamma + \mu + \sigma)} - 1\right]I_t \\
&\quad + [b_2\epsilon - b_1(\epsilon + \mu + \omega)]E_t.
\end{aligned}$$

Choosing $b_1 = \epsilon$, $b_2 = (\epsilon + \mu + \omega)$, it follows that:

$$\Delta F \leq b_2(\tau + \zeta + \gamma + \mu + \sigma)(\mathcal{R}_0 - 1)I_t.$$

Thus, $\Delta F \leq 0$ if $\mathcal{R}_0 \leq 1$., and $\Delta F = 0$ if $E_t = I_t = 0$. This indicates $(E, I) \to (0,0)$ as $t \to \infty$. Substituting $E = I = 0$ into the first and second equations of system (2.2), we find that $V \to \frac{\nu\Lambda}{\alpha+\mu}$ and $S \to \frac{(\alpha+\mu-\mu\nu)\Lambda}{\mu(\alpha+\mu)}$ as $t \to \infty$. This demonstrates that **DFE** is the maximal invariant set in $\{(V_t, S_t, E_t, I_t, D_t, X_t, T_t) : F_t = 0\}$. By Theorem 6.3 in [15], each solution associated with model (2.2), under the given initial conditions in Γ, converges to **DFE** as $t \to \infty$. □

5 Endemic-equilibrium

This section analyzes the existence and stability of an endemic equilibrium (**EE**) for model (2.2).

5.1 Existence of EE

The following lemma asserts the existence of **EE**.

Lemma 5.1. *For model (2.2), there exists a unique **EE**, if $\mathcal{R}_0 > 1$.*

Proof. At steady-state, the solution to the equations associated with system (2.2) yields:

$$V^{**} = \frac{\nu \Lambda}{(\alpha + \mu)},$$

$$S^{**} = \frac{(\epsilon + \mu + \omega)(\tau + \zeta + \gamma + \mu + \sigma)}{\beta \epsilon},$$

$$E^{**} = \frac{(\tau + \zeta + \gamma + \mu + \sigma)}{\epsilon} I^{**},$$

$$I^{**} = \frac{(\alpha + \mu - \mu \nu)\epsilon \Lambda}{(\alpha + \mu)(\epsilon + \mu + \omega)(\tau + \zeta + \gamma + \mu + \sigma)} - \frac{\mu}{\beta},$$

$$= \frac{\mu}{\beta}(\mathcal{R}_0 - 1),$$

$$D^{**} = \frac{\tau}{(\theta + \mu + \delta)} I^{**},$$

$$X^{**} = \frac{\zeta}{(\xi + \mu + \eta)} I^{**},$$

$$T^{**} = \left[\gamma + \frac{\omega(\tau + \zeta + \gamma + \mu + \sigma)}{\epsilon} + \frac{\theta \tau}{(\theta + \mu + \delta)} + \frac{\xi \zeta}{(\xi + \mu + \eta)} \right] I^{**}.$$

$\square$

5.2 Stability investigation of EE

The asymptotic stability of the unique **EE** is established in the following theorem:

Theorem 5.2. *The unique **EE** of model (2.2) is globally asymptotically stable (GAS) if $\mathcal{R}_0 \geq 1$ and $\mu \leq 1$.*

Proof. Consider the system (2.2). Furthermore, define the non-linear Lyapunov function:

$$U_t = \frac{1}{2} [(V_t - V^{**}) + (S_t - S^{**}) + (E_t - E^{**}) + (I_t - I^{**}) + (D_t - D^{**}) + (X_t - X^{**}) + (T_t - T^{**})]^2,$$

$$= \frac{1}{2} [(V_t + S_t + L_t + I_t + D_t + X_t + T_t) - (V^{**} + S^{**} + L^{**} + I^{**} + D^{**} + X^{**} + T^{**})]^2,$$

$$= \frac{1}{2}(N_t - N^{**})^2.$$

Calculating the backward difference of U_t gives:

$$\Delta U = U_{t+1} - U_t,$$
$$= \frac{1}{2}\left[(N_{t+1} - N^{**})^2 - (N_t - N^{**})^2\right],$$
$$= \frac{1}{2}(N_{t+1} - N_t)(N_{t+1} + N_t - 2N^{**}),$$
$$= -\frac{1}{2}(N_{t+1} - N_t)^2 + (N_{t+1} - N^{**})(N_{t+1} - N_t),$$
$$\leq (N_{t+1} - N^{**})(N_{t+1} - N_t).$$

Summing the equations of system (2.2) gives $N_{t+1} - N_t = \Lambda - (\sigma I^{**} + \delta D^{**} + \eta X^{**}) - \mu N_t$. At steady-state, $\Lambda - (\sigma I^{**} + \delta D^{**} + \eta X^{**}) = \mu N^{**}$, thus:

$$\Delta U = (N_t - \mu N_t + \mu N^{**} - N^{**})(\mu N^{**} - \mu N_t)$$
$$\leq (\mu^2 - \mu)(N_t - N^{**})^2.$$

Therefore, $\Delta U \leq 0$ if $\mu \leq 1$. Thus, **EE** is GAS if $\mathcal{R}_0 \geq 1$ and $\mu \leq 1$. $\qquad\square$

6 Data fitting for discrete model

In this section, estimates for seven model parameters will be derived by analyzing the WHO's Global Tuberculosis Report provides data on the incidence of tuberculosis (TB) cases world-wide [23], covering the years 2000 to 2022 (see Table 6.1). The statistical information found in the literature will be used to infer the remaining parameters. The death rate, denoted as μ, will be determined based on the average annual death rate from 2000 to 2022, using population data for India and Russia obtained from [19, 20].Similarly, as shown in Table 6.1, the number of births, Λ, will be computed as the mean annual birth rate from 2000 to 2022.

The total population of India was $N = 1\,059\,633\,675$ in 2000 [19]. Initial reported TB cases, $I_0 = 1\,115\,718$, were obtained from the World Health Organization [23]. The initial number of individuals with MDR and XDR was also obtained from [23].

The number of vaccinated individuals can be calculated as follows:

$$V_0 = \text{Number of births} \times \text{Vaccination rate.}$$

The assumed exposed individuals number is:

$$E_0 = 8\,852.$$

The assumed treated individuals number is:

$$T_0 = 2\,000.$$

Consequently, the initial susceptible population is determined as:

$$S_0 = N - (V_0 + E_0 + I_0 + D_0 + X_0 + T_0) = 851\,497\,070.$$

The initial conditions of the seven compartments of the discrete model for Russia were found to be the same as for India.

The child immunization rate, specifically the Bacillus Calmette-Guérin (BCG) vaccination rate, refers to the portion of children between 12 and 23 months who have received the BCG vaccination. This data is sourced from official statistics compiled by the World Bank [11, 12]. Therefore, the average vaccination rate, denoted as ν, can be calculated based on this information.

The treatment rate for MDR-TB (θ) can be given as the annual average treatment success rate for MDR-TB from 2000 to 2022. We have

Treatment success rate for MDR-TB for each year =

$$\frac{\text{Number of individuals who succeeded in treatment for MDR-TB each year}}{\text{Number of individuals with MDR-TB each year}}. \tag{6.1}$$

The treatment rate for XDR-TB, denoted as ζ, is determined as the average annual treatment success rate for XDR-TB observed from 2000 to 2022. We have

Treatment success rate for XDR-TB for each year =

$$\frac{\text{Number of individuals who succeeded in treatment for XDR-TB each year}}{\text{Number of individuals with XDR-TB each year}}. \tag{6.2}$$

The disease death rate in MDR-TB (δ) can be given as the annual average death rate in MDR-TB from 2000 to 2022. We have

Death rate in MDR-TB for each year =

$$\frac{\text{Number of individuals who died due to MDR-TB each year}}{\text{Number of individuals with MDR-TB each year}}. \tag{6.3}$$

The disease death rate in XDR-TB (η) can be given as the annual average death rate in XDR-TB from 2000 to 2022. The death rate in XDR-TB for each year is given by:

Death rate in XDR-TB for each year =

$$\frac{\text{Number of individuals who died due to XDR-TB each year}}{\text{Number of individuals with XDR-TB each year}}. \tag{6.4}$$

The estimated values of $\beta, \gamma, \epsilon, \sigma, \omega, \tau, \alpha,$ and ζ are obtained by minimizing the difference between the exact solution of the suggested model (2.2) and the incidence data on TB.

$$\Phi = \sum_{i=1}^{n}(I_{t_i} - I_{t_i}^*)^2, \tag{6.5}$$

where $I_{t_i}^*$ represents the observed TB infected cases at time t_i and I_{t_i} is the corresponding model-predicted value. n here represents the total number of data points that are available. The objective function 6.5 was minimized using the Levenberg-Marquardt algorithm and the MATLAB function `fitnlm`.

Figures 6.1, 6.2 illustrate the tuberculosis (TB) incidence data for Russia and India , respectively, alongside the model-fitted curves generated using the parameter estimates provided in Table 6.1.
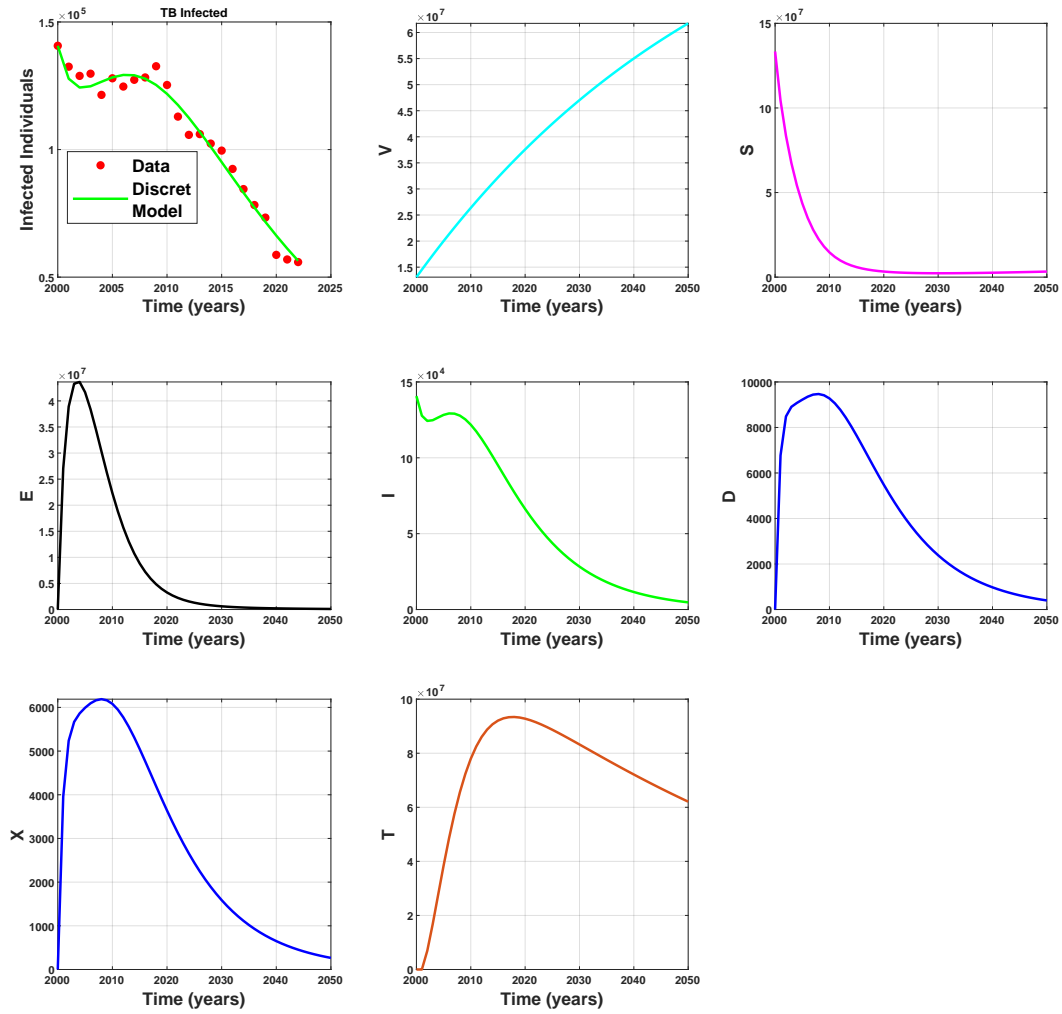
Figure 6.1: TB incidence data and model fit for Russia, where the data is shown in green and the fitted model is depicted in red. The basic reproduction number $\mathcal{R}_0 = 0.22 < 1$.
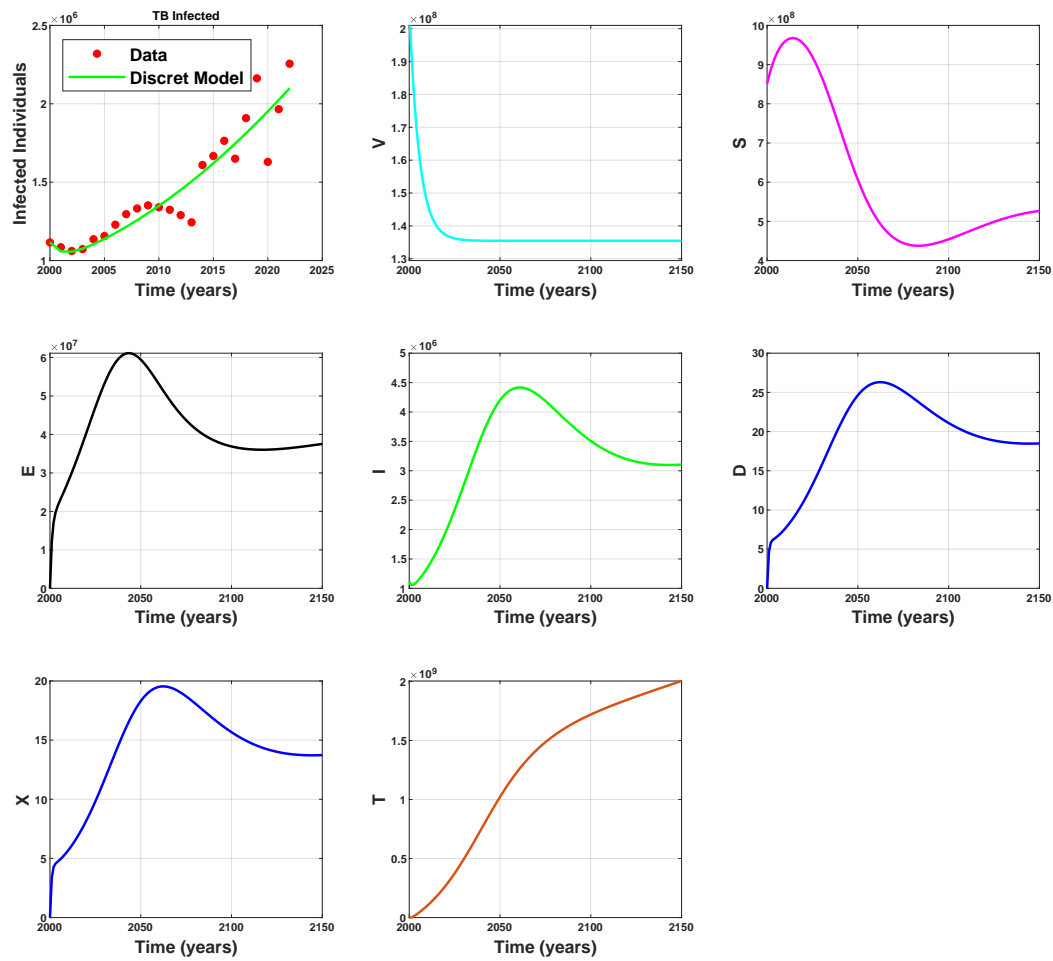
Figure 6.2: TB incidence data and model fit for India, where the data is shown in green and the fitted model is depicted in red. The basic reproduction number $\mathcal{R}_0 = 6.42 > 1$.

Table 6.1: Model parameters and initial conditions for Russia and India.

Parameters	Russia parameters	References	India parameters	References
$V(0)$	$13,791,833$	[12]	$180,967,005$	[11]
$S(0)$	$132,653,507$	Calculated	$851,497,070$	Calculated
$E(0)$	$8,852$	Assumed	$8,852$	Assumed
$I(0)$	$140,677$	[23]	$1,115,718$	[23]
$D(0)$	0	[23]	0	[23]
$X(0)$	0	[23]	0	[23]
$T(0)$	$2,000$	Assumed	$2,000$	Assumed
Λ	$1,720,142.287$	[20]	$26,469,994.76$	[19]
μ	0.015	[20]	0.007	[19]
ν	0.96	[12]	0.858	[11]
α	0.0012	Fitted	0.160	Fitted
β	1.45×10^{-6}	Fitted	1.27×10^{-8}	Fitted
γ	1×10^{-14}	Fitted	0.043	Fitted
ϵ	0.0003	Fitted	0.004	Fitted
ω	0.254	Fitted	0.542	Fitted
τ	0.048	Fitted	4.17×10^{-6}	Fitted
ζ	0.028	Fitted	3.02×10^{-6}	Fitted
ξ	0.36	Calculated [23]	0.356	Calculated [23]
θ	0.49	Calculated [23]	0.504	Calculated [23]
δ	0.15	Calculated [23]	0.189	Calculated [23]
σ	2.81×10^{-6}	Fitted	0.006	Fitted
η	0.21	Calculated [23]	0.319	Calculated [23]

7 Analyzing the sensitivity of $\mathcal{R}_0$

The analysis of the sensitivity of the fundamental reproduction number $\mathcal{R}_0$ vs model parameters is determined in this section. To begin with, we get the partial derivatives of the fundamental reproduction number vs the model parameters $\beta,\gamma,\epsilon,\omega,\tau,\zeta,\sigma,\alpha,\mu,\nu$. The associated partial derivatives are calculated using the following definition:

Definition 7.1. The normalized sensitivity index of $\mathcal{R}_0$ dependent on the differentiability on a parameter ρ:

$$S_\rho^{\mathcal{R}_0} = \frac{\rho}{\mathcal{R}_0} \frac{\partial \mathcal{R}_0}{\partial \rho}.$$

The following partial derivatives are based on the definition from above:

$$S_\beta^{\mathcal{R}_0} = \frac{\beta}{\mathcal{R}_0} \frac{\partial \mathcal{R}_0}{\partial \beta} = 1 > 0,$$

$$S_\gamma^{\mathcal{R}_0} = \frac{\gamma}{\mathcal{R}_0} \frac{\partial \mathcal{R}_0}{\partial \gamma} = \frac{-\gamma}{(\gamma + \mu + \sigma + \tau + \zeta)},$$

$$S_\epsilon^{\mathcal{R}_0} = \frac{\epsilon}{\mathcal{R}_0} \frac{\partial \mathcal{R}_0}{\partial \epsilon} = 1 - \frac{\epsilon}{(\omega + \epsilon + \mu)},$$

$$S_\omega^{\mathcal{R}_0} = \frac{\omega}{\mathcal{R}_0} \frac{\partial \mathcal{R}_0}{\partial \omega} = \frac{-\omega}{(\omega + \epsilon + \mu)},$$

$$S_\tau^{\mathcal{R}_0} = \frac{\tau}{\mathcal{R}_0} \frac{\partial \mathcal{R}_0}{\partial \tau} = \frac{-\tau}{(\gamma + \mu + \sigma + \tau + \zeta)},$$

$$S_\zeta^{\mathcal{R}_0} = \frac{\zeta}{\mathcal{R}_0} \frac{\partial \mathcal{R}_0}{\partial \zeta} = \frac{-\zeta}{(\gamma + \mu + \sigma + \tau + \zeta)},$$

$$S_p^{\mathcal{R}_0} = \frac{p}{\mathcal{R}_0} \frac{\partial \mathcal{R}_0}{\partial \nu} = \frac{-(\mu\nu)}{(\alpha + \mu - \mu\nu)},$$

$$S_\alpha^{\mathcal{R}_0} = \frac{\alpha}{\mathcal{R}_0} \frac{\partial \mathcal{R}_0}{\partial \alpha} = \frac{(\alpha\mu\nu)}{((\alpha + \mu)(\alpha + \mu - \mu\nu))},$$

$$S_\sigma^{\mathcal{R}_0} = \frac{\sigma}{\mathcal{R}_0} \frac{\partial \mathcal{R}_0}{\partial \sigma} = \frac{-\sigma}{(\gamma + \mu + \sigma + \tau + \zeta)},$$

$$S_\mu^{\mathcal{R}_0} = \frac{\mu}{\mathcal{R}_0} \frac{\partial \mathcal{R}_0}{\partial \mu} = -\left(\frac{\mu}{(\gamma + \mu + \sigma + \tau + \zeta)} + \frac{\mu}{(\omega + \epsilon + \mu)} + \frac{\mu}{(\alpha + \mu)} + 1 + \frac{\mu((\nu - 1))}{(\alpha + \mu - \mu\nu)} \right).$$

Table 7.1: Sensitivity index for the basic reproduction number $\mathcal{R}_0$.

Parameters	sensitivity index
μ	-1.6712
ν	-9.5533
α	$+0.5449$
β	$+1$
γ	-6.8240×10^{-14}
ϵ	$+0.9963$
ω	-0.9759
τ	-0.5153
ζ	-0.3788
σ	-1.1943×10^{-04}

8   Numerical results

The parameter estimation results are summarized in Table 6.1. The TB incidence data are displayed alongside the model-fitting curve in Figures 6.1, 6.2, which were fitted using Table 6.1's parameter values. The model demonstrates a strong fit, as evidenced by high coefficients of determination, $\mathcal{R}^2 = 0.8709$ for India and $\mathcal{R}^2 = 0.977$ for Russia. These values indicate that the model effectively captures the observed patterns in the real data.

Using the estimated parameter values, the calculated $\mathcal{R}_0$ is 6.42 for India (greater than 1), indicating that the **DFE** is unstable, while the $\mathcal{EE}$ is asymptotically stable, as shown in Figure 6.2. Conversely, for Russia, the calculated $\mathcal{R}_0$ is 0.22 (less than 1), suggesting that the **DFE** is asymptotically stable, while $\mathcal{EE}$ is unstable, as illustrated in Figure 6.1.

To further explore how specific parameters influence disease spread, Figures 8.1, 8.2 depict graphical representations of R_0 versus ten parameters. The basic reproduction number $\mathcal{R}_0$ shows a strong positive association with β, α, and ϵ. This indicates that an increase in these parameters leads to a higher $\mathcal{R}_0$, facilitating greater disease transmission.

Conversely, an inverse relationship is observed between $\mathcal{R}_0$ and the remaining parameters $\gamma, \nu, \tau, \zeta, \omega, \sigma$, and μ. Higher values of these parameters correspond to a lower $\mathcal{R}_0$, which indicates a slower spread of the disease. These insights are consistent with real-world observations.
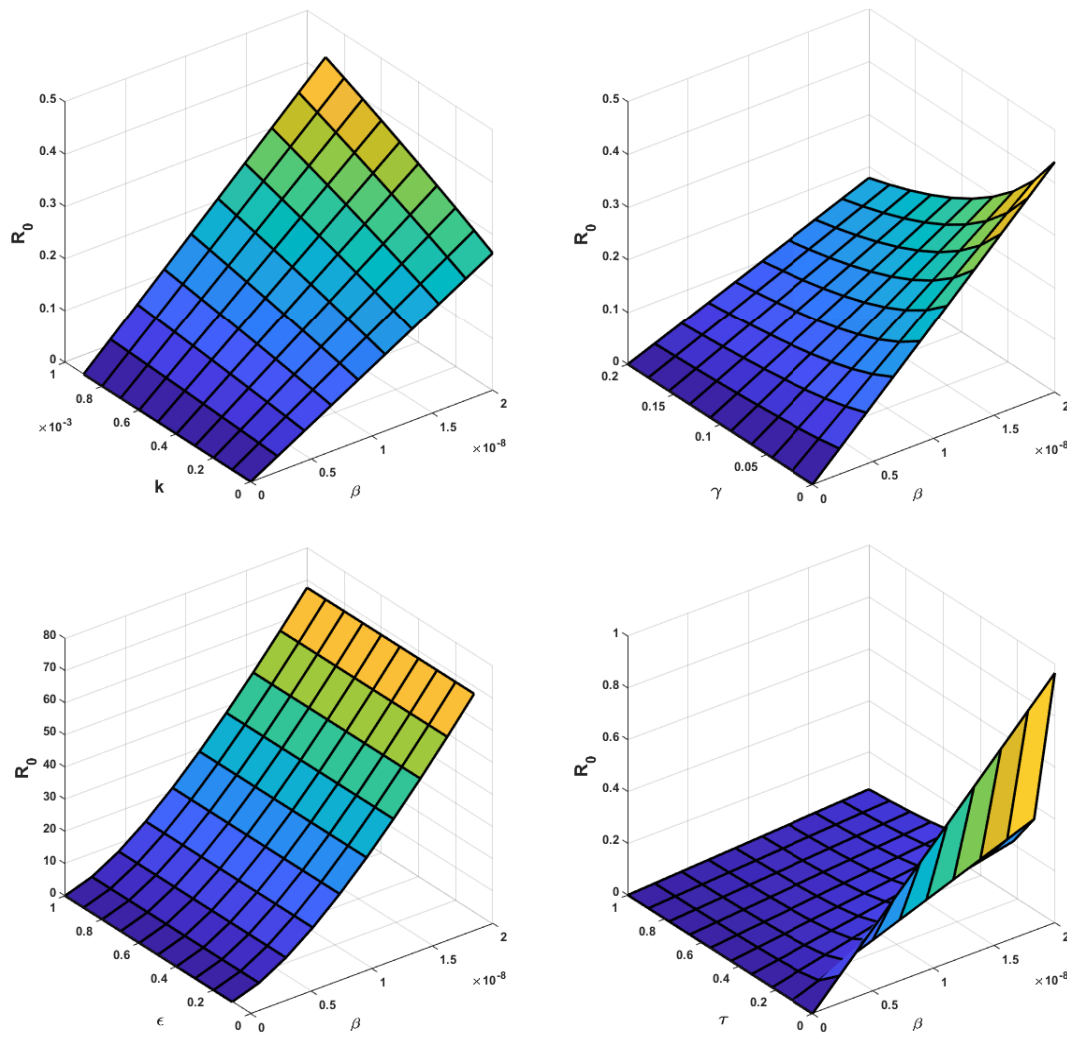
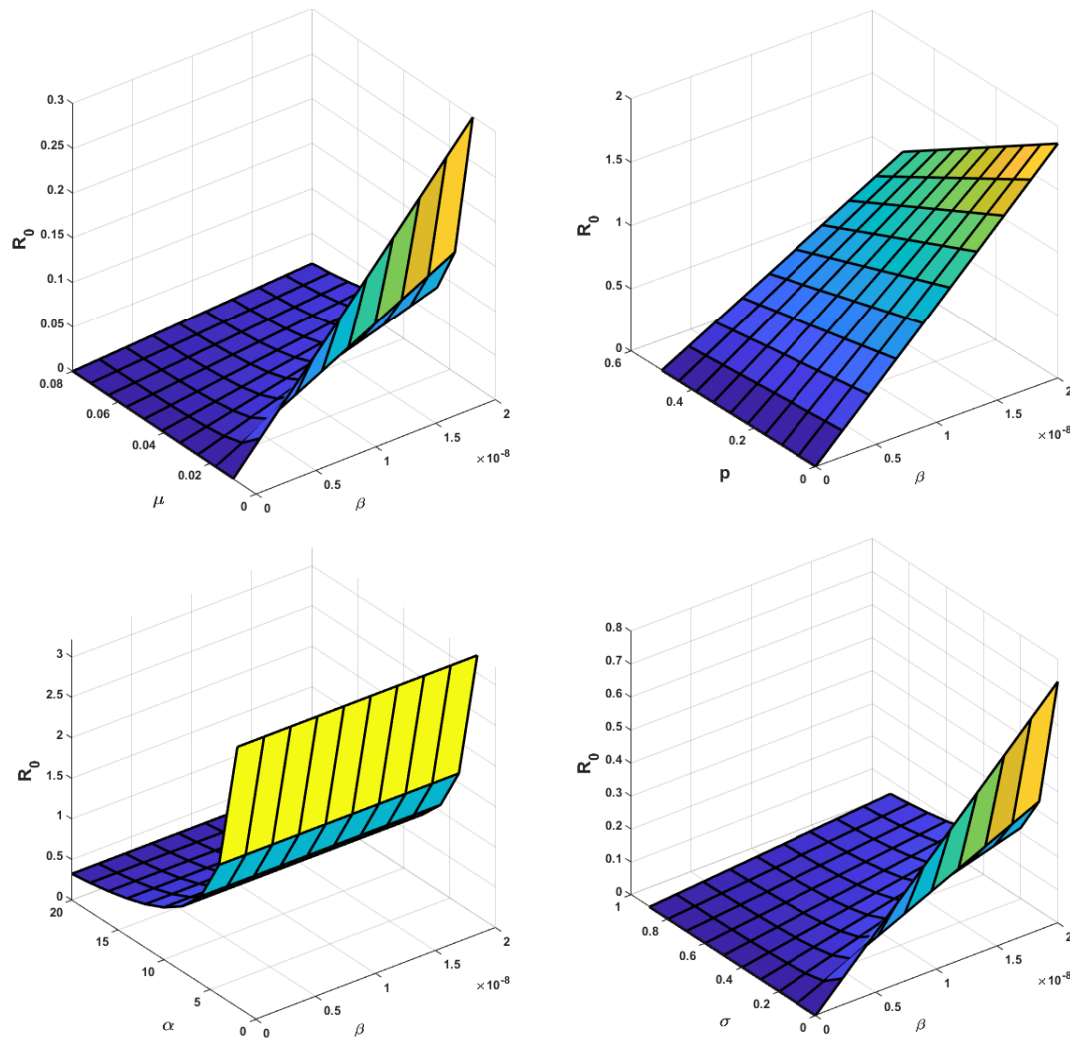Figure 8.1: Representation of $\mathcal{R}_0$ versus $\beta, \tau, \gamma, \epsilon$ and α.

Figure 8.2: Representation of $\mathcal{R}_0$ versus $\beta, \nu, \omega, \sigma$, and μ.

The initially presented model by Gupta et al. [9] did not take into account the impact of chemoprophylaxis for individuals with latent TB infection, nor did consider the effects of treatment for those with active TB disease. However, to improve upon this, D. B. Kitaro et al. [14] attempted to enhance the model by including chemoprophylaxis treatment for latent infections and treatment for individuals with active TB. Consequently, this study focused on parameter estimation and demonstrated the impact of chemoprophylaxis and vaccination on the infected, **MDR**, and **XDR** classes. The analysis utilized incidence data from India and Russia to assess the effectiveness of these interventions.

By examining Figure 8.3, it becomes apparent the number of individuals in the infected categories, **MDR** and **XDR**, lacking chemoprophylaxis treatment surpasses those receiving such treatment among the exposed groups. Furthermore, with an increase in the chemoprophylaxis treatment parameter ω, it becomes evident that administering chemoprophylaxis to Exposed individuals significantly curbs the transmission of tuberculosis.
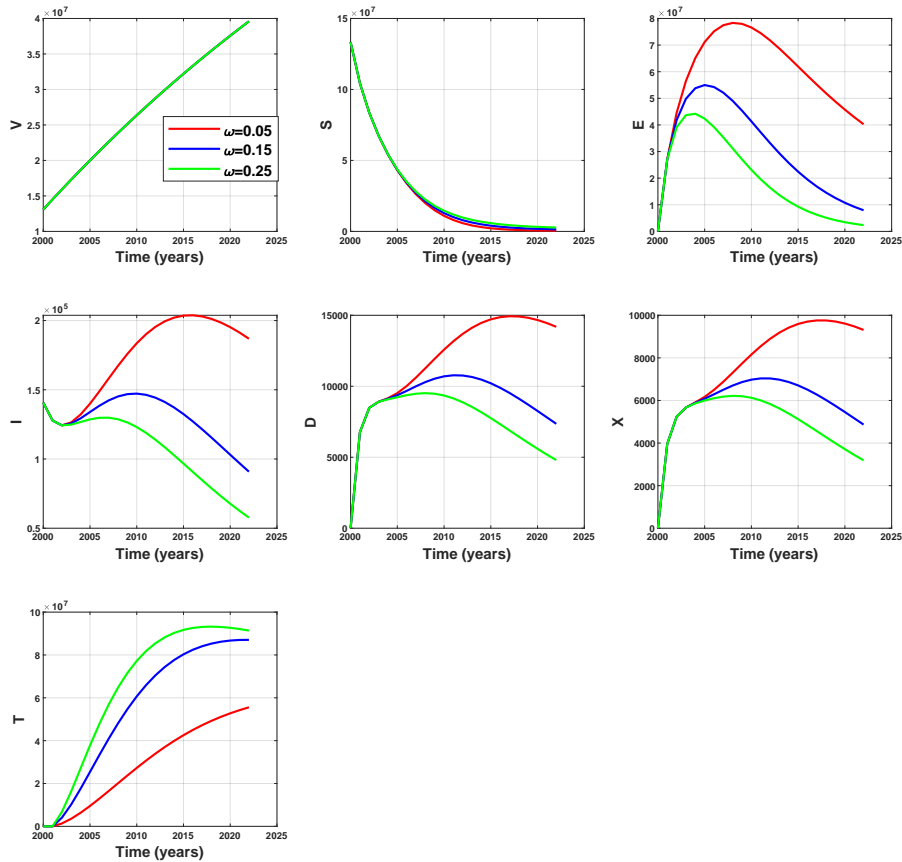
Figure 8.3: Effect of the chemoprophylaxis treatment rate on the compartemants of the discrete model (2.2).

In Figure 8.4, the decrease in the infected, **MDR**, and **XDR** classes with an increase in BCG vaccination rate can be explained by the protective effects of the vaccine. BCG (Bacillus Calmette-Guérin) is a vaccine primarily used against TB and is known to provide partial protection against certain strains of the bacteria that cause TB.

When more individuals receive the BCG vaccine, it creates a higher level of immunity within the population. This increased immunity makes it more difficult for the TB bacteria, including **MDR**, and **XDR** strains, to infect individuals who have been vaccinated. As a result, the spread of these drug-resistant strains is reduced, leading to a decrease in the number of infected individuals within these classes.

In summary, the effectiveness of BCG vaccination in reducing the prevalence of **MDR-TB**, and **XDR-TB** strains is demonstrated by the inverse relationship between vaccination rate and the size of these infected classes depicted in Figure 8.4.

Overall, the numerical investigation provide evidence that the inclusion of the parameter ω of chemoprophylaxis treatment and vaccination rate ν in the model leads to a more effective reduction in the transmission of TB, particularly in cases involving **MDR**, and **XDR** compartments. This improvement is observed in contrast to the model that lacks chemoprophylaxis treatment for Exposed individuals and vaccination rate.
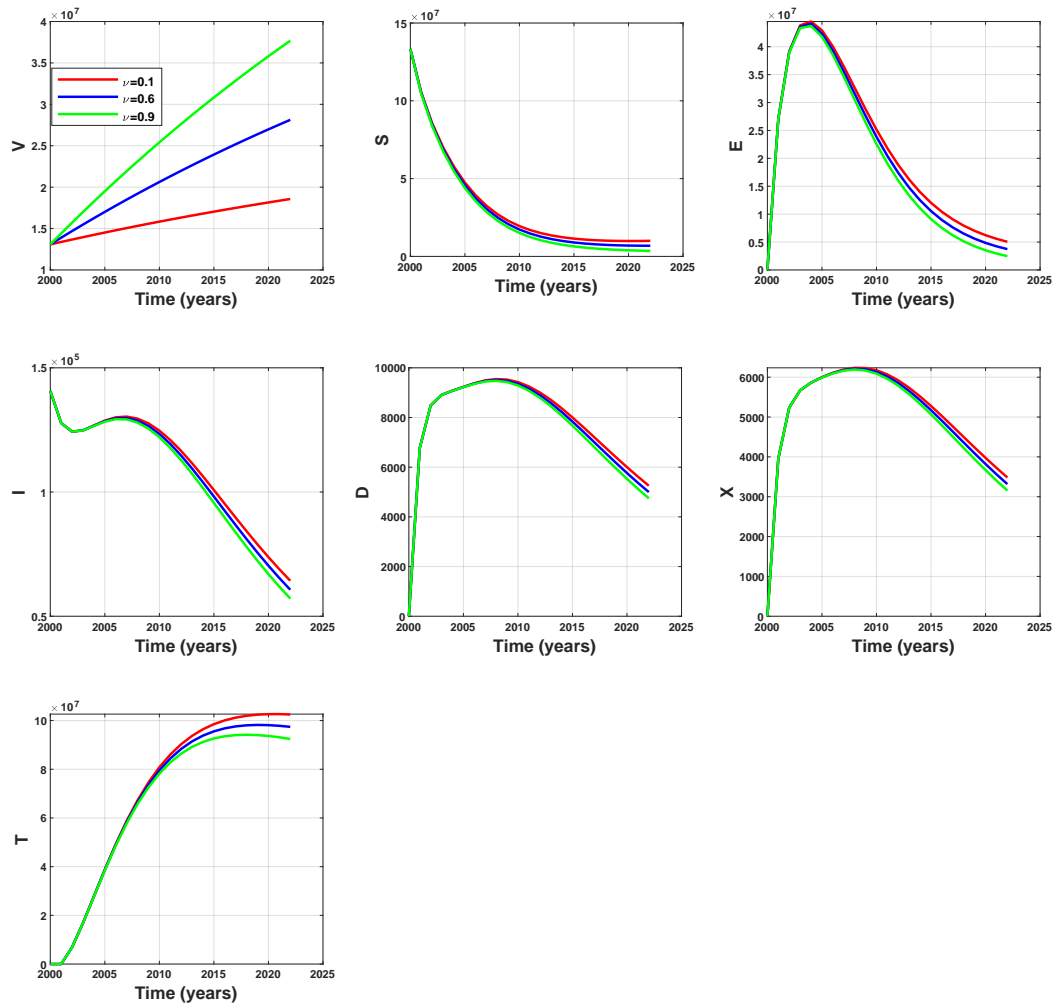
Figure 8.4: Effect of the vaccination rate on the compartments of the discrete model (2.2).

Figure 8.5 illustrates a comparison between the discrete model and the continuous model, concerning the number of infected cases in Russia. The discrete model exhibits a good fit, evidenced by a high coefficient of determination value of $\mathcal{R}^2 = 0.98$. However, the coefficient of determination for the continuous model, $\mathcal{R}^2 = 0.93$, is lower than that of the discrete model.
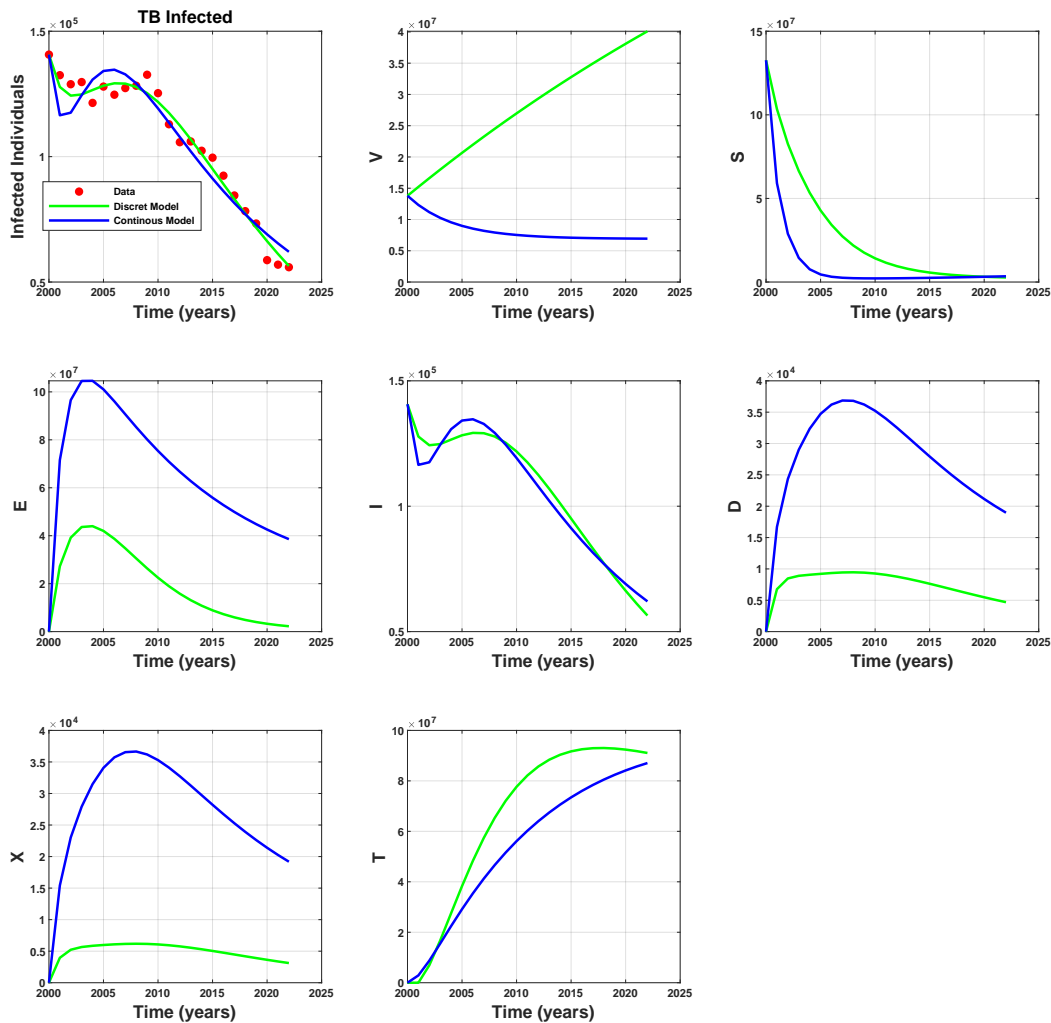
Figure 8.5: Comparision of the discrete model and continuous model vs Russia's Data.

The discrete model fits better because its structure is well-suited to capturing the dynamics of time-stepped data, particularly when the data is collected in discrete intervals, such as daily case counts. Additionally, if the real-world data has inherent discrete properties or exhibits abrupt changes over time, the discrete model can naturally accommodate these variations more effectively. Furthermore, discrete models are more flexible in capturing nonlinear behaviors and sudden changes, such as bifurcations, leading to a more accurate representation of the observed data.

9   Conclusion

This research developed and analyzed a discrete mathematical model of TB transmission, focusing on MDR-TB and XDR-TB cases. The model, adapted from a continuous-time framework using the Euler forward method with a step size of $h = 1$, incorporates the effects of chemoprophylaxis for the Exposed group and vaccination rates. The study used the next-generation matrix principle to calculate the basic reproduction ratio, $\mathcal{R}_0$, and analyzed the model's characteristics, including the stability of disease-free and endemic equilibrium points.

By adjusting the model parameters with actual TB incidence data from India and Russia, the research estimated $\mathcal{R}_0$ as 6.42 for India and 0.22 for Russia, indicating a higher risk of TB transmission in India. The model's predictions aligned well with actual TB cases, suggesting its potential for forecasting the disease's future status. Sensitivity analysis revealed that increasing chemoprophylaxis for exposed individuals reduces transitions to MDR and XDR states, while BCG vaccination improves immunity and decreases transmission. Given TB's higher prevalence in India compared to Russia, urgent actions are recommended, including enhanced treatment, better healthcare facilities, and widespread educational campaigns to reduce TB impact in India.

Declarations

Availability of data and materials

Data sharing not applicable to this article.

Funding

Not applicable.

Conflict of interest

The authors have no conflicts of interest to declare.

Acknowledgements

We want to thank the two reviewers for their valuables comments.

References

[1] L. J. ALLEN, *Some discrete-time SI, SIR, and SIS epidemic models*, Mathematical Biosciences, **124**(1) (1994), 83–105. URL

[2] L. J. ALLEN, AND A. M. BURGIN, *Comparison of deterministic and stochastic SIS and SIR models in discrete time*, Mathematical Biosciences, **163**(1) (2000), 1–33. URL

[3] R. M. ANDERSON, AND R. M. MAY, Population Biology of Infectious Diseases. *Report of the Dahlem workshop on population biology of infectious disease agents Berlin 1982*, Berlin: Springer Science and Business Media, 2012. URL

[4] F. BRAUER, Z. FENG, AND C. CASTILLO-CHAVEZ, *Discrete epidemic models*, Mathematical Biosciences and Engineering, **7**(1) (2009), 1–15. URL

[5] F. A. CHALUB, AND M. O. SOUZA, *Discrete and continuous SIS epidemic models: a unifying approach*, Ecological Complexity, **18** (2014), 83–95. URL

[6] B. CHENNAF, M. S. ABDELOUAHAB, AND R. LOZI, *Analysis of the Dynamics of Tuberculosis in Algeria Using a Compartmental VSEIT Model with Evaluation of the Vaccination and Treatment Effects*, Computation, **11**(7) (2023), 146. URL

[7] Z. Chen, *Discrete-time vs. continuous-time epidemic models in networks*, IEEE Access, **7** (2019), 127669–127677. URL

[8] O. Diekmann, J. A. P. Heesterbeek, and J. A. Metz, *On the definition and the computation of the basic reproduction ratio R0 in models for infectious diseases in heterogeneous populations*, J. Math. Biol, **28** (1990), 365–382. URL

[9] V. K. Gupta, S. K. Tiwari, S. Sharma, and L. Nagar, *Mathematical model of tuberculosis with drug resistance to the first and second line of treatment*, Journal of New Theory, (2018), 94106. URL

[10] H. W. Hethcote, *The mathematics of infectious diseases*, SIAM Review, **42**(4) (2000), 599–653. URL

[11] Trading Economics. Immunization, BCG (% Of One-year-old Children) India, Available online:
https://tradingeconomics.com/india/immunization-bcg-percent-of-one-year-old-children-wb-data.html

[12] World Health Organization. Immunization, BCG (% Of One-year-old Children) Russia, Available online:
https://apps.who.int/gho/data/view.main.80500?lang=en

[13] G. Izzo, A. Vecchio, *A discrete time version for models of population dynamics in the presence of an infection*, Journal of Computational and Applied Mathematics, **210**(1-2) (2007), 210–221. URL

[14] D. B. Kitaro, B. K. Bole, and K. P. Rao, *Mathematical Analysis of Tuberculosis Transmission Model with Multidrug and Extensively Drug-resistance Incorporating Chemoprophylaxis Treatment*, Jambura J. Math, **6**(1) (2024), 1–10. URL

[15] J. P. LaSalle, An invariance principle in the theory of stability, in: *Differential Equations and Dynamical Systems (Proc. Internat. Sympos., Mayaguez, P. R., 1965)*, Academic Press, New York, 1967, 277–286. URL

[16] X. Li, and W. Wang, *A discrete epidemic model with stage structure*, Chaos, Solitons and Fractals, **26**(3) (2005), 947–958. URL

[17] R. E. Mickens, *Discretizations of nonlinear differential equations using explicit nonstandard methods*, Journal of Computational and Applied Mathematics, **110**(1) (1999), 181–185. URL

[18] C. Porwal, A. Kaushik, N. Makkar, J. N. Banavaliker, M. Hanif, R. Singla,... and U. B. Singh, *Incidence and risk factors for extensively drug-resistant tuberculosis in Delhi region*, PLoS One, **8**(2) (2013), e55299. URL

[19] Population growth in India, Available online:
https://www.donneesmondiales.com/asie/inde/croissance-population.php

[20] Population growth in Russia, Available online:
https://www.donneesmondiales.com/europe/russie/croissance-population.php

[21] M. Ronoh, R. Jaroudi, P. Fotso, V. Kamdoum, N. Matendechere, J. Wairimu,... and J. Lugoye, *A mathematical model of tuberculosis with drug resistance effects*, Applied Mathematics, **7**(12) (2016), 1303–1316. URL

[22] R. Ross, *The prevention of malaria*, J. Murray, (1910). URL

[23] WHO. Global tuberculosis report. *World Health Organization*, Available online: https://extranet.who.int/tme/generateCSV.asp?ds=notifications

[24] P. Van den Driessche, and J. Watmough, *Reproduction numbers and sub-threshold endemic equilibria for compartmental models of disease transmission*, Mathematical Biosciences, **180**(1-2) (2002), 29–48. URL

[25] H. Waaler, A. Geser, and S. Andersen, *The use of mathematical models in the study of the epidemiology of tuberculosis*, American Journal of Public Health and the Nations Health, **52**(6) (1962), 1002–1013. URL

[26] G. Yeni, E. Akn, and N. K. Vaidya, *Time scale theory on stability of explicit and implicit discrete epidemic models: applications to Swine flu outbreak*. Journal of Mathematical Biology, **88**(1) (2024), 6. URL

[27] World Health Organization. Available online: https://www.who.int/news-room/fact-sheets/detail/tuberculosis

[28] World Health Organization. *Extensively drug-resistant tuberculosis (XDR-TB): recommendations for prevention and control*, Weekly Epidemiological Rec, **81**(45) (2006), 430–432.